Formation of satellite bands in the ionization spectra of extended systems

Michaël S. Deleuze* and Lorenz S. Cederbaum
Lehrstuhl für Theoretische Chemie, Institut für Physikalische Chemie, Universität Heidelberg, D69120 Heidelberg, Germany
(Received 6 December 1995)

The ionization spectra of hydrogen clusters converging onto a polymer limit have been investigated by means of one-particle Green's-function calculations. This study focuses on the construction of well-organized correlation bands of shake-up satellites at the expense of the lines in the main (primary) band. Two series of chains have been studied, belonging, in regards to their fundamental Hartree-Fock band gap, to the categories of insulating and semiconducting polymers. Evidence is given for a limitation of the contamination by shake-up lines with the delocalization properties of one-particle canonical states in an insulating situation, whereas a nearly complete fragmentation of main bands into satellites can be expected with polymers of the semiconducting type, as a result of multistates interactions. The onset of this contamination, marking in the ionization spectrum a bifurcation between the one-particle and correlation regimes, can be evaluated from a zeroth-order estimate for the energy threshold of a shake-up transition. Electronic correlation in the neutral ground-state wave function is also shown to increase the breakdown of the one-particle picture of ionization. [S0163-1829(96)06919-6]

I. INTRODUCTION

Extensive theoretical work on the photoionization spectra of polymers has been conducted since the 1970's based on the assumption of a one-particle picture for the ionization process, implying a one-to-one correspondence between the recorded lines and canonical states computed at various methodological levels. Among others these methods comprise the extended Hückel[1] or Hartree-Fock Roothaan[2] approaches, and the numerous intermediate methods based[3] on a semiempirical one-particle Hamiltonian-like zero differential overlap (ZDO), complete neglect of differential overlap (CNDO), intermediate neglect of differential overlap (INDO), modified neglect of differential overlap (MNDO), . . . or more recently VeH (valence effective Hamiltonian).[4] A major aspect of photoelectron spectroscopy, to be largely credited to the benefit of these investigations, is that it tends today to be commonly exploited as a direct and very specific probe[2,5–8] of the molecular architecture (bonding characteristics, configuration, conformation) of complex compounds or clusters in the gas, liquid, and solid phases. Owing to the development of powerful experimental techniques using e.g., synchrotron radiation of electron beams as excitation sources, on the one hand, and on the other hand to a growing interest in investigations on the superficial structure of advanced materials such as polymer microcrystals[2,7,8] or self-assembled organic layers,[9] quantum chemists and physicists encounter more frequently than ever demands for accurate simulations of valence photoionization spectra. These simulations have to include electronic correlation and relaxation effects, as well as the subsequent dispersion of intensity from the main bands into satellite structures of shake-up lines.

Several experimental[10] and theoretical[5,7,11,12] investigations have pointed out strong correlation and reorganization effects on the position and intensity of the primary peaks, and disclosed in the more acute situations strong evidences for a severe breakdown of the one-particle picture of ionization.[11] The photoionization intensity originating from inner electron levels has been found in many situations, including the rather gentle case of the weakly correlated saturated hydrocarbons,[13] to be spread out over many shake-up lines of comparable strength, as a result of strong configuration interactions (CI's) within the cation.

Experimental x-ray photoionization spectra have recently displayed spectacular evidence[14] for the dominant role played by correlation bands in the ionization spectra of conjugated polyenes related to polyacetylene. Relatedly, a splitting of the 3σ band of polyacetylene into several satellite (shake-up) bands has been qualitatively inferred[15] from crystal orbital calculations including hole-mixing effects at the lowest (second) order of a perturbation expansion in terms of the correlation potential. As a general shortcoming of any second-order method, however, the breakdown of the one-particle picture remains, in this case, confined to the edges of the first Brillouin zone and in the lower half part of the inner valence region.

Going beyond a strict second-order expansion with respect to correlation, further investigations[16] have been conducted on the very first terms of the polyacene series, $C_{2n}H_{2n+2}$, with $n=2$, 3, 4 and 5, using CI schemes restricted to the $1h$ (one hole) and $2h$-$1p$ (two holes, one particle) configurations of the cation. For the longest chains ($n=4$ or 5), additional restrictions on excitations have been imposed in the form of a projection of the virtual states onto the canonical valence space generated by a minimal basis set, in so-called $2h$-$1v$ CI calculations. These calculations have proved convincingly a complete contamination of the spectrum of polyacetylene by satellite lines up to the low-energy border of the outer valence region, in roughly good agreement with experiment. As pointed out by the authors of this investigation, however, the applied CI schemes suffer from too serious theoretical drawbacks to confidently allow for a quantitative assignment of the shake-up peaks. The neglect of electronic correlation in the reference wave function, first, might yield an erroneous sequence of ionic states in compounds with low symmetry and virtual states at low energy. Furthermore, the loss of size consistency with the truncation of the excitation space spanned by the Hamiltonian leads

certainly to a severe underestimation of many-body effects for the largest systems with respect to the smallest ones.

A basic postulate of band-structure theory in solid-state physics is the organization of one-electron levels in regular energy distributions (i.e., one-particle *bands*) for extended systems exhibiting translational symmetry. Owing to this postulate, the one-particle band structure of stereoregular polymers is often determined by extrapolating the results of one-particle calculations on oligomers of increasing size. It is clear that shake-up lines in the ionization spectrum of large but finite periodic systems should similarly fall in densely packed but well-organized energy distributions, to be directly related to satellite bands in crystal orbital calculations[15] on the corresponding polymer. However, because of the complexity of the compounds addressed and owing to the rapidly growing number of shake-up solutions with respect to oligomer size, no regular energy distributions clearly emerged from the spectral densities displayed in Ref. 16. Besides the construction of correlation bands, a clear relationship between the shake-up spreading and the energy separation between the valence and conduction bands was also left, even at a qualitative level, as a very challenging question.

In this contribution, we take advantage of the simplicity and flexibility of the model of a polymer form of hydrogen and follow in an oligomer series the construction of correlation bands and their dependence to geometrical features, using one of the most powerful and reliable instruments for the analysis of ionization process: the one-particle Greens'-function method.[17–21] This scheme has been the object of various approximations, derived by a linearization of the equations of motion, using the algebraic superoperator formalism,[22] or by an infinite order analysis[23,24] of Feynman diagrams. In the realm of extended systems, these approaches offer, in comparison with a standard CI treatment, the combined advantages of error cancellations in energy differences, systematic *compactness*[24,25] of the configuration space in high-order approximations, and *energy separability* with respect to[26] dissociation of a large system into noninteracting fragments (*size consistency*). The latter feature relates[26] to the topological linked-cluster properties[28–30] of any many-body perturbation expansion based on the Dyson evolution operator, and is a necessary prerequisite[26,27,31] for a correct (*size-intensive*) scaling of the computed transition energies and moments with respect to system size. When dealing with long-range electron-electron interactions in large systems, however, a true size-intensivity of the one-particle Green's function is also[31] determined by the N representability of the computed electron density.

This paper is organized as follows. Section II consists of a review of the major properties of the one-particle Green's function and of the successive steps for its evaluation in the framework of an algebraic diagrammatic construction (ADC) scheme, in the outlook of numerical applications on extended systems. In Secs. III and IV use is made of two series of hydrogen chains to follow in insulating and semiconducting situations the competition between main and satellite lines in the ionization spectra of clusters converging onto a polymer limit. Geometrical variations are also considered to evaluate on a semiquantitative level the conditions which lead to a significant contamination of the main band by correlation lines.

II. THE ONE-PARTICLE GREEN'S FUNCTION AND ITS EVALUATION

Defined as a time-ordered expectation value of a creation (a_j^+) and an annihilation (a_i) operators in Heisenberg representation on the exact N-particle ground state $|\Psi_0^N\rangle$, the one-particle Green's function is the simplest member in the hierarchy of Green's functions. As an autocorrelation function,[32] it gives the probability amplitude of propagation in a correlated background of an extra electron or hole in between one-particle states, during a given time interval (t_1,t_2):

$$G_{ij}(t_2,t_1)=i^{-1}\langle\Psi_0^N|T\{a_i(t_2),a_j^+(t_1)\}|\Psi_0^N\rangle. \tag{1}$$

In most applications, the operator basis is spanned by a discrete set of one-particle states ϕ_i obtained as the ground-state one-particle [Hartree-Fock (HF)] orbitals. The importance of the one-particle Green's function for the evaluation of electronic structure effects in condensed matter physics can be readily appreciated from its spectral representation in the energy space, which for an N-particle system with a nondegenerate (closed-shell) ground state takes the form

$$G_{ij}(\omega)=\sum_{n\in\{N+1\}}\frac{\langle\Psi_0^N|a_i|\Psi_n^{N+1}\rangle\langle\Psi_n^{N+1}|a_j^+|\Psi_0^N\rangle}{\omega+E_0^N-E_n^{N+1}+i\eta}+\sum_{n\in\{N-1\}}\frac{\langle\Psi_0^N|a_j^+|\Psi_n^{N-1}\rangle\langle\Psi_n^{N-1}|a_i|\Psi_0^N\rangle}{\omega+E_n^{N-1}-E_0^N-i\eta}, \tag{2}$$

where η is a positive infinitesimal introduced to ensure the convergence of the Fourier transform coupling the time and energy representations of G. In this equation, $|\Psi_n^{N\pm1}\rangle$ and $E_n^{N\pm1}$ are the exact $(N\pm1)$-particle states and energies, respectively. E_0^N represents the energy of the exact neutral ground state $|\Psi_0^N\rangle$. The first (retarded) and second (advanced) parts of $G(\omega)$ bear essential information on the electron attachment (or scattering) and ionization processes, respectively. The (vertical-electronic) ionization energies, $I_n=E_n^{N-1}-E_0^N$, and electron affinities, $A_n=E_0^N-E_n^{N+1}$, can be derived from the location of the poles of $G(\omega)$ in the upper and lower half planes, respectively, of the complex energy plane. The associated residues correspond to products of transition amplitudes:

$$x_i^{(n)}=\begin{cases}\langle\Psi_0^N|a_i|\Psi_n^{N+1}\rangle & \forall\quad n\in\{N+1\}\\ \langle\Psi_n^{N-1}|a_i|\Psi_0^N\rangle & \forall\quad n\in\{N-1\},\end{cases} \tag{3}$$

which are closely related to spectroscopic intensities. When molecular-orbital cross-section effects are neglected, as will be the case here, the partial pole strengths $\gamma_{\rm in}=|x_i^{(n)}|^2$ are most conveniently merged into a global spectroscopic factor $\Gamma_n=\Sigma_i\gamma_{\rm in}$, giving an estimate of the fraction of photoemission intensity related to a one-particle process. The remaining fraction $1-\Gamma_n$ is the intensity dispersed in correlation and relaxation effects. Pole strengths close to unity refer to a one-particle process, while small pole strengths are indicative of a breakdown of the one-particle picture.[11]

The exact one-particle Green's function for a many-body system is traditionally expanded through a renormalization[17,29,30] of a suitable zeroth-order form over an effective energy-dependent potential, the so-called irreducible self-energy $\Sigma(\omega)$, by means of the Dyson equation:

$$G(\omega)=G^{(0)}(\omega)+G^{(0)}(\omega)\Sigma(\omega)G(\omega). \tag{4}$$

In practice, the zeroth-order (free) Green's function is most frequently defined with respect to the uncorrelated HF particles:

$$G_{ij}^{(0)}=\delta_{ij}\left(\frac{n_i}{\omega-\epsilon_j-i\eta}+\frac{\overline{n_i}}{\omega-\epsilon_i+i\eta}\right). \tag{5}$$

In this equation, ϵ_i represents the HF orbital energies, and $n_i=1-\overline{n_i}$ denote the HF ground-state occupation numbers.

The dynamic self-energy is usually written as the sum[19,33]

$$\Sigma(\omega)=\Sigma(\infty)+M(\omega), \tag{6}$$

where the dynamic (energy-dependent) part $M(\omega)$ accounts for the long-time scale many-body effects arising within the $N\pm1$-particle systems, whereas, owing to a Fourier transform, the static (energy-independent) part $\Sigma(\infty)$ corresponds to many-body processes, which occur instantaneously. In the energy representation, the latter component relates to the electrostatic potential felt by an ingoing or outgoing particle due to correlation corrections to the HF ground-state density

$$\Sigma_{pq}(\infty)=\sum_{kl}\langle\phi_p\phi_k||\phi_q\phi_l\rangle[\rho_{lk}^{\text{exact}}-\rho_{lk}^{\text{HF}}], \tag{7}$$

where $\langle\phi_p\phi_k||\phi_q\phi_l\rangle$ denote antisymmetrized bielectron integrals over spin orbitals.

As $G(\omega)$, the dynamic self-energy separates naturally into two independent parts, that are physically associated with excitations of the $(N+1)$- and $(N-1)$-particle systems, according to

$$M(\omega)=M^{+}(\omega)+M^{-}(\omega). \tag{8}$$

Each of these components possesses an analytical structure similar to the energy representation of the one-particle Green's function. Using matrix representation techniques, both can be developed using the exact algebraic form[24]

$$M_{pq}^{\pm}(\omega)=(U_p^{\pm})^{\dagger}(\omega-K^{\pm}-C^{\pm})^{-1}U_q^{\pm}. \tag{9}$$

In this equation, the effective energy interactions $K^{\pm}+C^{\pm}$ and coupling amplitudes $U_q^{\pm}$ are defined with respect to shake-on and shake-up configuration spaces of the $(N+1)$- and $(N-1)$-particle systems, respectively. In the algebraic approximation, these spaces are spanned by the physical $(N\pm1)$-particle excitations derived within the basis of the N-particle ground-state Hartree-Fock orbitals. The matrices $K^{\pm}$ are diagonal and correspond to a zeroth-order (i.e., HF) estimate of the shake-on and shake-up energies, respectively. In the so-called algebraic diagrammatic construction (ADC) scheme,[23,24] finite-order expressions [ADC (2), ADC (3), ADC (4)] for the requested energy shifts $C^{\pm}$ and coupling amplitudes $U_q^{\pm}$ have been derived by comparison with diagrammatic perturbation expansions of $M^{\pm}(\omega)$ through the required order. At the second-order and third-order levels, strictly equivalent expressions have also been obtained by means of a direct expansion[22] of the one-particle propagator, using the equation-of-motion (EOM)/algebraic superoperator approach.

As contrasted with a finite-order expansion of the self-energy, infinite partial geometrical series in powers of the energy shift $C^{\pm}$ are automatically included by virtue of the matrix inverse in Eq. (9), which thereby accounts for collective excitations, an essential feature for the investigation of electronic structure effects in extended systems. In the ADC formulation, the influence of electron correlation in the ground state on the dynamic polarization effects induced by ionization is also accounted for, from third order and beyond, by the vectors of coupling amplitudes $U_q^{\pm}$.

Once the energy shifts $C^{\pm}$ and coupling amplitudes $U_q^{\pm}$ have been computed, the dynamic self-energy can be readily transformed into a suitable diagonal form,

$$M_{pq}^{\pm}(\omega)=\sum_{\mu\in\{N\pm1\}}\frac{m_p^{\pm(\mu)}m_q^{\pm(\mu)*}}{\omega-\omega_\mu^{\pm}\pm i\eta}, \tag{10}$$

by solving, independently from each others, the eigenvalue problems:

$$(K^{+}+C^{+})Y^{+}=Y^{+}\Omega^{+},\quad (Y^{+})^{\dagger}Y^{+}=1^{+}$$

$$(K^{-}+C^{-})Y^{-}=Y^{-}\Omega^{-},\quad (Y^{-})^{\dagger}Y^{-}=1^{-}, \tag{11}$$

in which the pole positions $\omega_\mu^{\pm}$ of $M^{\pm}(\omega)$ are found as the eigenvalues contained in $\Omega^{\pm}$, whereas the corresponding Feynman-Dyson amplitudes are obtained according to

$$m_p^{\pm(\mu)}=(U_p^{\pm})^{\dagger}Y^{\pm(\mu)}. \tag{12}$$

A basic property of the ADC scheme, which is important for numerical applications on extended systems, concerns the size of the configuration spaces. In contrast to a conventional CI treatment, where the Coulomb matrix elements enter the CI expansions exclusively in linear form, the explicit ADC (n) space extends only[24,25] with each even order n, ensuring a greater *compactness* of the required matrices. At third-order, for example, only the $2p$-$1h$ (two particle, one hole) and $2h$-$1p$ (two holes, one particle) excitations are needed to span the configuration spaces of the $N\pm1$-particle systems, respectively, whereas a comparable CI expansion would in addition also require the $3p$-$2h$ (three particles, two holes) and $3h$-$2p$ (three holes, two particles) configurations. Furthermore, unlike a CI expansion, the ADC equations are manifestly *size consistent*, since they relate to a linked-cluster expansion. In a localized picture, this means that these equations decouple into independent (local) sets for a system consisting of noninteracting fragments, ensuring the required separability properties for size-intensive properties. Turning alternatively to a delocalized picture, size consistency can also be inferred[26] from a correct balance between the delocalization and multiplicity of one-particle canonical states.

Since only the eigenvalues and eigenvectors in the ionization sector of $G(\omega)$ have to be extracted, one can take advantage of the independence of the $(N+1)$- and $(N-1)$-particle blocks of the dynamic self-energy and of the fact that these blocks are energetically located far apart from each

other. This allows one to replace the $(N+1)$ block, of usually very large dimension, by a much smaller matrix, which mimics perfectly the behavior of the $(N+1)$ block in the ionization region.[34] Instead of truncating this block by a selection of the more important configurations, a crude approximation which may seriously affect the accuracy of the final results, use has been made[34] of projection methods based on a block (or band) extension[35,36] of the Lanczos algorithm.[37] After L iteration steps of this algorithm, the $K^+ + C^+$ block is reduced to a L-dimensional tridiagonal matrix,

$$t = V^\dagger (K^+ + C^+) V, \tag{13}$$

where V is the matrix of Lanczos vectors. Diagonalizing further this matrix according to

$$tZ = Z\widetilde{\Omega}^+, \quad Z^\dagger Z = 1 \tag{14}$$

provides a pseudospectrum of L approximate eigenvalues $\widetilde{\omega}_\mu = \widetilde{\Omega}_{\mu\mu}$ for the $K^+ + C^+$ matrix. The accompanying approximate coupling Dyson amplitudes are obtained via back transformation, as

$$\widetilde{m}_p^{+(\mu)} = (U_p^+)^\dagger V Z^{(\mu)}. \tag{15}$$

This method has made the ADC (3) calculations much faster and feasible on large systems, without loss of accuracy.[34]

In practical applications, the efficiency of the one-particle propagator method is ultimately determined by $\Sigma(\infty)$, which is known to influence rather seriously the accuracy of the results obtained for the single-hole ionic states, as it enters sensitively the Dyson equation (4). In the ADC formulation, the correlated part of the electron density from which the static self-energy is derived is itself evaluated[38,39] through partial contour integrations over a suitable truncated form of the Dyson expansion for $G(\omega)$. The problem of determining $\Sigma(\infty)$ reduces, therefore, to a single matrix inversion,

$$\Sigma_{pq}(\infty) - \sum_{kl} \langle \phi_p \phi_k || \phi_q \phi_l \rangle \frac{n_l \overline{n_k} - \overline{n_l} n_k}{\epsilon_l - \epsilon_k} \Sigma_{pq}(\infty) = b_{pq}, \tag{16}$$

entirely defined in the space of the one-particle and one-hole configurations. Here, the major numerical obstacles arise from the inhomogeneities,

$$b_{pq} = \sum_{kl} \langle \phi_p \phi_k || \phi_q \phi_l \rangle Q_{lk}, \tag{17}$$

requiring the evaluation of the correlated part of the one-electron density, according to

$$Q_{lk} = Q_{lk}^+ + Q_{lk}^- \tag{18}$$

$$Q_{lk}^+ = \sum_{\mu \in \{N+1\}} m_l^{+(\mu)} m_k^{+(\mu)*} \left\{ \frac{-n_l n_k}{(\epsilon_k - \omega_\mu^+)(e_l - \omega_\mu^+)} + \frac{n_k \overline{n_l}}{(\epsilon_k - \epsilon_l)(\epsilon_k - \omega_\mu^+)} + \frac{n_l \overline{n_k}}{(\epsilon_l - \epsilon_k)(\epsilon_l - \omega_\mu^+)} \right\},$$

$$Q_{lk}^- = \sum_{\mu \in \{N-1\}} m_l^{-(\mu)} m_k^{-(\mu)*} \left\{ \frac{\overline{n_l n_k}}{(\epsilon_k - \omega_\mu^-)(\epsilon_l - \omega_\mu^-)} + \frac{n_l \overline{n_k}}{(\epsilon_l - \epsilon_k)(\epsilon_k - \omega_\mu^-)} + \frac{n_k \overline{n_l}}{(\epsilon_k - \epsilon_l)(\epsilon_l - \omega_\mu^-)} \right\}.$$

As with the dynamic part of the self-energy, one can exploit the Lanczos pseudoeigenspectrum and the related approximate coupling Dyson amplitudes for the $N+1$-particle, block by inserting the results of Eqs. (14) and (15) into (18) to simplify the evaluation of Q^+. Q^-, on the other hand, has been determined using the inversion method described in Ref. 39.

A last difficulty resides in the size dependence of $\Sigma(\infty)$, the diagonal elements of which may diverge logarithmically[31] with the size of a stereoregular chain, as a result of a violation of the particle number[40] with the correlation corrections to the one-electron density:

$$\Delta N = \mathrm{tr}(Q). \tag{19}$$

When dealing with molecular systems of relatively small size, this error has very little influence on the computed results. To avoid this problem, which could on the other hand impede seriously the reliability of conclusions drawn for extended (not necessarily infinite) systems, use has been made in Eq. (17) of a properly rescaled form of the correlated one-electron density, reevaluated[31] as

$$\widetilde{Q}_{lk} = \frac{N}{N + \Delta N} \left[Q_{lk} - n_l \delta_{lk} \frac{\Delta N}{N} \right], \tag{20}$$

which preserves the total particle number as $\mathrm{tr}(\widetilde{Q}) = 0$.

Once the static self-energy has been computed, the Dyson equation is ultimately recast into the following CI-like eigenvalue problem:[34]

$$AX = XE, \quad X^\dagger X = 1, \tag{21}$$

together with

$$A = \begin{pmatrix} \epsilon + \Sigma(\infty) & \widetilde{m}^+ & m^- \\ (\widetilde{m}^+)^\dagger & \widetilde{\Omega}^+ & 0 \\ (m^-)^\dagger & 0 & \Omega^- \end{pmatrix}, \tag{22}$$

in which the results of the Lanczos diagonalization (14) and (15) for the electron affinity block have been explicitly inserted. After solving (21) via diagonalization, the poles $\omega_n = E_0^N - E_n^{N-1}$ and residue amplitudes $x_i^{(n)} = \langle \Psi_n^{N-1} | a_i | \Psi_0^N \rangle$ of $G(\omega)$ are readily derived from the eigenvalues $e_n = E_{nn}$ and the corresponding eigenvector components X_{in}, respectively, of the matrix A.

III. MODELS AND COMPUTATIONAL DETAILS

Modeling stereoregular polymers by linear or cyclic hydrogen chains has proved on many occasions[41] to be very useful for investigating electronic structure effects in condensed-matter physics, such as electron-electron and electron-lattice interactions, Peierls distortion, or metal-insulator transition. In the field of conducting polymers, owing to an intrinsic trend to a symmetry-breaking alternation

TABLE I. Fundamental gap (ΔE_g) of the selected chains, versus their length (NH: number of hydrogen atoms) and bond-length alternation.

NH	Alternation	ΔE_g (eV)
(a)		
4	1.4/1.5	17.649
8	1.4/1.5	12.710
12	1.4/1.5	10.094
16	1.4/1.5	8.411
20	1.4/1.5	7.210
24	1.4/1.5	6.290
28	1.4/1.5	5.548
(b)		
4	1.4/1.8	19.722
8	1.4/1.8	16.274
12	1.4/1.8	14.708
16	1.4/1.8	13.839
20	1.4/1.8	13.304
24	1.4/1.8	12.951
28	1.4/1.8	12.705
32	1.4/1.8	12.527
36	1.4/1.8	12.394
40	1.4/1.8	12.293
(c)		
28	1.4/1.5	5.548
28	1.4/1.6	10.562
28	1.4/1.7	11.716
28	1.4/1.8	12.705
28	1.4/1.9	13.573
28	1.4/2.0	14.332

of the electron density, equidistant hydrogen chains have frequently served as simple prototypes of conjugated polyenes based on polyacetylene. Interestingly, such chains provide also a one-dimensional model for certain solid metallic phases of hydrogen[42] existing in high-pressure and low-temperature conditions.

In this work, extrapolations to the polymer limit are drawn from ADC (3) calculations carried out using a 3-21-G basis, on two series of finite hydrogen chains of increasing size, with alternating bond lengths of 1.4 and 1.8 a.u., or 1.4 and 1.5 a.u. (1 a.u.$=0.529\,18$ Å). These geometrical parameters have been selected in order to obtain (Table I) fundamental band gaps comparable to those found at the HF level for, respectively, all-trans polyethylene (16.17 eV using a 6–31 G* basis[43]), a typical insulator, and for all-trans polyacetylene (5.14 eV, using a 6–31 G** basis[44]), a polymer conventionally classified as a semiconductor in its undoped form. Geometrical structure effects on the ionization spectra have been also evaluated by considering a third series of calculations, using a few other interdistances between hydrogen atoms (see Table I).

The self-consistent-field computations have been carried out using the GAMESS series of programs.[45] The requested convergence on each of the elements of the density matrix and the integral cutoff were fixed to 10^{-5} and 10^{-9} hartree, respectively. The Green's-function results have been obtained by means of the ADC code[24,34] described in the preceding section. Only the poles with a spectroscopic strength larger than 0.005 have been extracted from the eigenvalue equation (21). The spatial symmetry has been exploited to the extent of the largest one-dimensional (Abelian) subgroup D_{2h} of the full symmetry group $D_{\infty h}$, to construct symmetry-adapted configurations and decouple the eigenvalue problem (21) into lower-dimensional problems for each irreducible representation.

IV. RESULTS

A. Size dependence of correlation bands

The size dependence of the location and intensity of main and satellite lines can be followed in Figs. 1(a) and 2(a), in which the ADC (3) values obtained for binding energies and the corresponding spectroscopic strengths have been displayed as three-dimensional spike spectra. Hypothetical ionization spectra have been correspondingly simulated in Figs. 1(b) and 2(b), using as a convolution function a combination of one Lorentzian and one Gaussian function, both having the same height and width (1.2 eV at half the maximum). In these convolutions, to illustrate more clearly the size dependence of shake-up bands, we display separately the spectral contribution arising from the lines with a pole strength smaller than an arbitrary threshold of 0.40.

When running through the series of insulating hydrogen chains with bond lengths of 1.4 and 1.8 a.u., the pole strength distributions [Fig. 1(a)] and the corresponding convoluted spectra [Fig. 1(b)] converge rather quickly to their respective asymptotic profiles. In this case, one can readily discriminate the main band from its correlation tail. Except for one or two lines at the bottom of the ionization spectrum, pole strengths in the main band remain larger than 0.78, showing that, in an insulating case, the one-particle picture for the ionization process is essentially well-preserved over the whole valence region. As observed with less sophisticated propagator calculations on the same systems,[27] pole strengths tend to decrease continuously with increasing binding energy, as a result of an exaltation of electronic pair relaxation effects[22a] induced by ionization of the deepest levels. These effects relate to the advanced (hole) sector of the self-energy, and are related in the Heidelberg's school as correlation effects in the final state.[11] Some contamination by shake-up lines is observed in the high-binding-energy part of the main band, in a region characterized by the highest density of one-electron states. This overall behavior is typically that found for saturated chains.[7,11j,13,46]

Only one satellite of rather low intensity ($\Gamma_n=0.10$) contributes to the spectrum of the smallest chain considered here (H_4). When one extends the length of the chain, this shake-up splits into a rapidly growing number of states, which dissolves into a quasicontinuum of solution of very small spectroscopic strength (typically less than 0.05). The correlation tail covers interestingly the largest energy interval for the medium-sized chains (H_{12}, H_{16}, H_{20}), extending from 15.0 eV up to about 36 eV, and then retreats for the longest systems (H_{36}, H_{40}) in a domain below 30 eV. Relatedly, the more intense shake-up lines are also found for the (H_{12}, H_{16}, and H_{20}) chains. This behavior is reminiscent of the size-dependence properties of the orbital relaxation contributions evaluated at second order on the same hydrogen

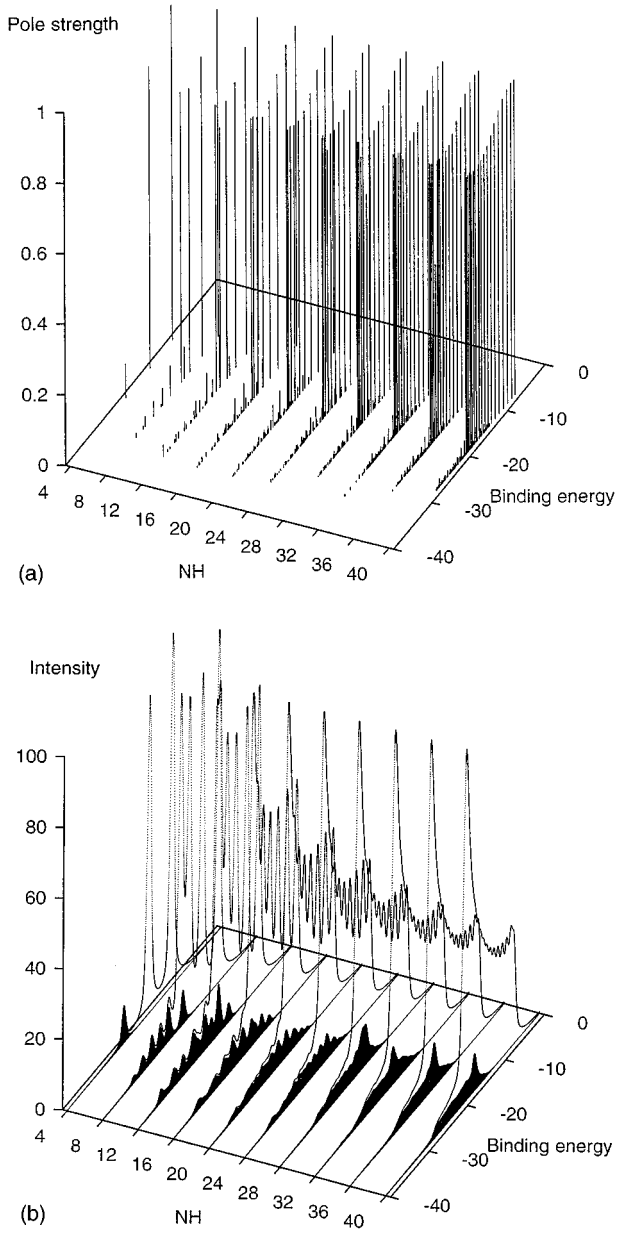

FIG. 1. Size dependence of (a) the pole strength profile and (b) convoluted photoionization spectrum (FWHM=1.2 eV) of insulating hydrogen chains (alternating bond lengths of 1.4 and 1.8 a.u.), together with the contribution due to the lines characterized by a pole strength factor smaller than 0.40, superimposed as shaded spectra. NH represents the number of hydrogen atoms.

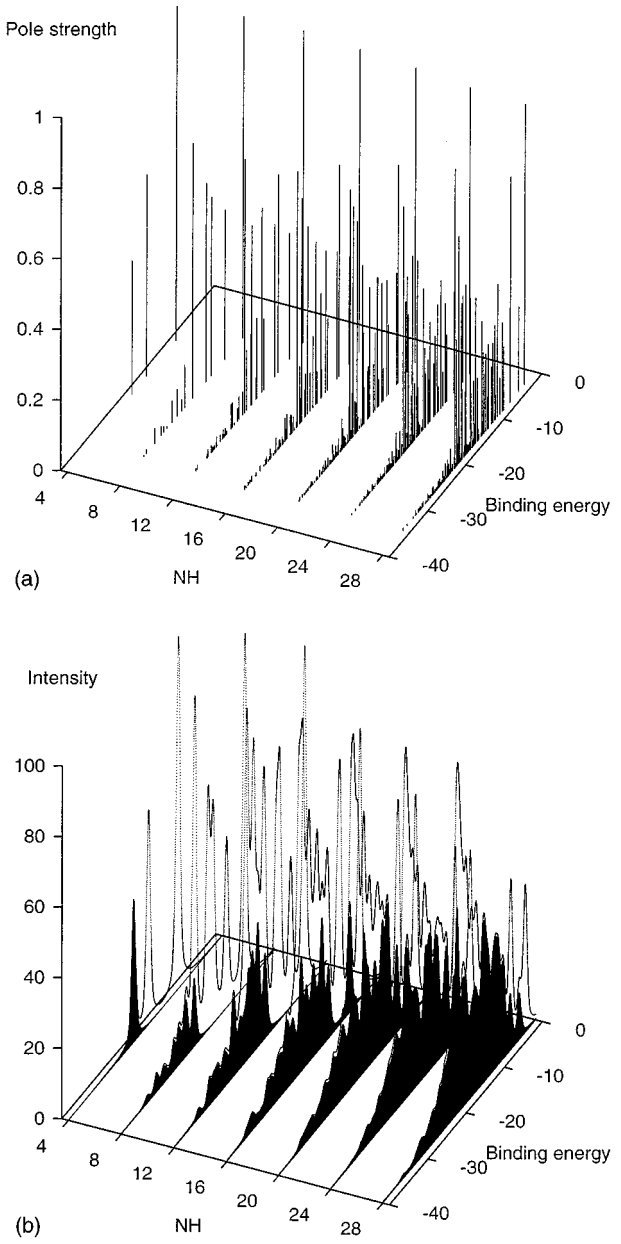

FIG. 2. Size dependence of (a) the pole strength profile and (b) convoluted photoionization spectrum (FWHM=1.2 eV) of semiconducting hydrogen chains (alternating bond lengths of 1.4 and 1.5 a.u.), together with the contribution due to the lines characterized by a pole strength factor smaller than 0.40, superimposed as shaded spectra.

chains,[27] and therefore certainly relates to an identical cause, namely, the $(N_0)^{-1}$ size-dependence properties of bielectron integrals over canonical orbitals delocalized over the whole system, with N_0 the number of unit cells in the chain. Like bielectron integrals, the first- and second-order amplitudes coupling primary states to the shake-up (shake-on) configuration subspace of the $N-1$ $(N+1)$ particle system become vanishingly small in the longest chains, a trend which, in systems with a wide gap, tends to thwart the multiplication of satellite solutions.

As contrasted with insulating hydrogen chains, for which the correlation tail remains small and confined at the high-energy border of the main band, the much more pronounced metallic character of the chains with 1.4 and 1.5 a.u. leads to a nearly complete fragmentation [Fig. 2(a)] of the main band into a very complex set of shake-up lines, except for a few lines at the high- and low-energy borders of the main band. This fragmentation can be traced up to the smallest chain H_4, for which a splitting of the first occupied electron level into two lines of comparable strength ($\Gamma_n=0.379$ and $\Gamma_{n'}=0.573$) is already observed. Accordingly, much of the spectrum of the longest semiconducting chains consists of a huge and poorly structured correlation bump, extending nearly over the whole valence region, from 6.0 up to 35.0 eV. Beyond 20

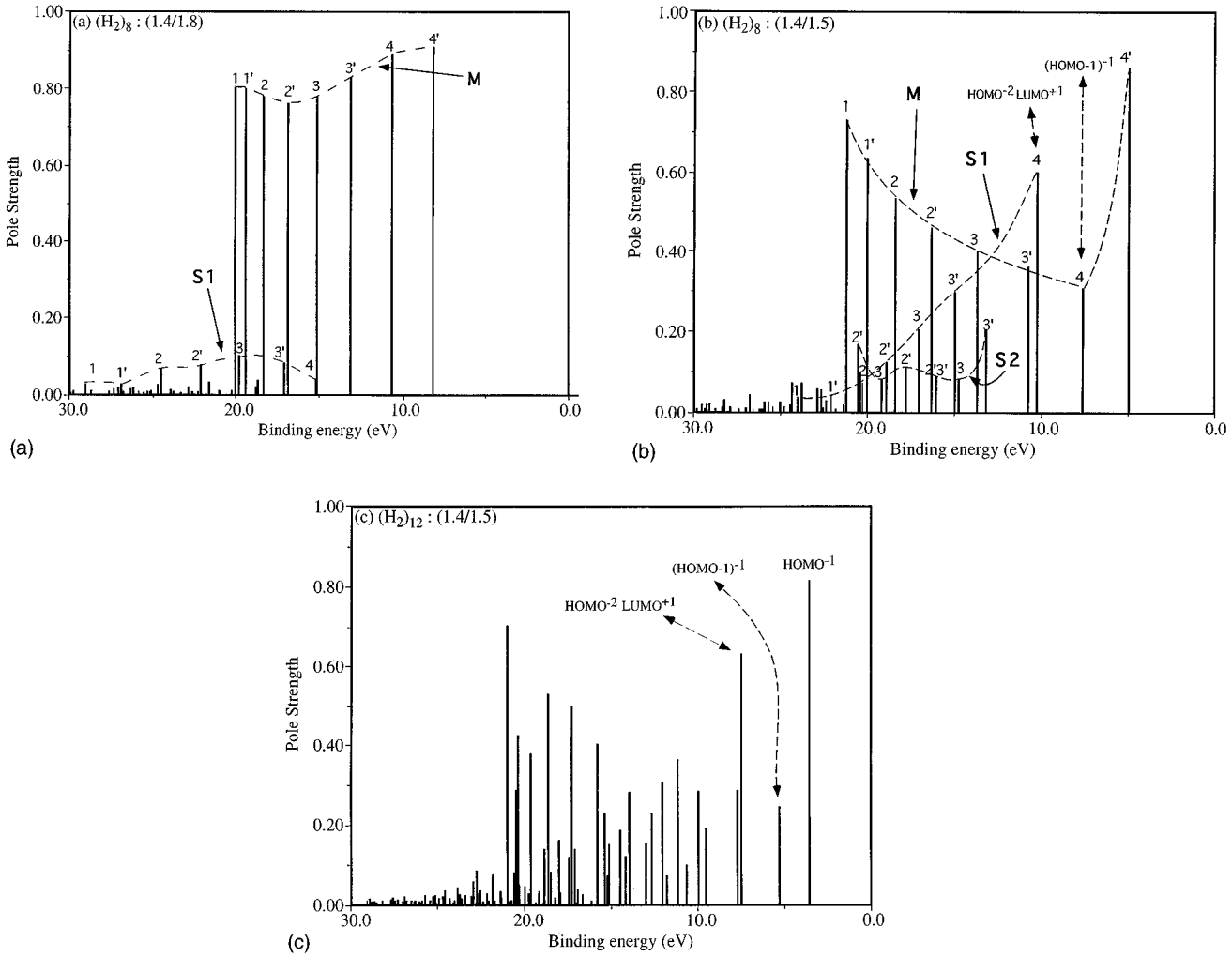

FIG. 3. Detailed analysis of the ionization spectrum of (a) an insulating or (b) a semiconducting H_{16} hydrogen chain, with alternating bond lengths of 1.4 and 1.8 a.u., or 1.4 and 1.5 a.u., respectively, in terms of regular bands. Dotted lines are included as a guide to the eye, to distinguish regular bands. In this figure, the main band (M) relates to single-hole lines, whereas satellite bands of shake-up lines, $S1$ and $S2$, are the result of $1h/2h\text{-}1p$ and $2h\text{-}1p/2h\text{-}1p$ configuration interactions, respectively. The lines in these bands are labeled according to the leading contribution arising in the $1h$ part of the corresponding eigenvector, indicating therefore the molecular orbital from which they originate (a primed label relates to an antisymmetric orbital, whereas symmetric orbitals are denoted using unprimed labels). The overall structure of (b) is retained for the spectrum (c) of a larger H_{24} chain with alternating bond lengths of 1.4 and 1.5 a.u. (HOMO: highest occupied molecular orbital; LUMO: lowest unoccupied molecular orbital; HOMO-1: the occupied molecular orbital below the HOMO.)

eV, the pole strength profile and the shape of the correlation tail saturate rather quickly to their asymptotic form, whereas around 10 eV the band attributed to correlation is far from having converged to the polymer limit.

B. Organization of shake-up lines into regular bands

Both in the insulating and semiconducting cases, the leading shake-up lines tend clearly to fall into rather well-organized bands, as illustrated in Figs. 3(a) and 3(b) for a small hydrogen chain (H_{16}), and as one should expect from translational symmetry requirements. In these figures, one can easily identify the eight lines contributing to the main band (M) of the H_{16} chain, which are labeled according to their molecular-orbital index. One regular distribution ($S1$) of shake-up lines also clearly emerges from the spectrum of the (H_{16}) chain with bond lengths of 1.4 and 1.8 a.u. [Fig. 3(a)]. These lines are labeled according to the one-electron levels from which they borrow their intensity, as indicated from the composition of the corresponding eigenvector obtained solving equation (21). Taking the terminology used in crystalline orbital calculations[15] on extended periodic systems, the splitting displayed in Fig. 3(a) can be regarded as a prelude to the construction of a regular satellite (or correlation) band of rather weak intensity for the corresponding polymer. Similarly, two regular bands of shake-up lines, $S1$ and $S2$, can be readily identified in the ionization spectrum of the H_{16} chain with bond lengths of 1.4 and 1.5 a.u. [Fig. 3(b)]. Owing to the much more pronounced metallic character of this chain, these bands account this time for a major part of the intensity.

Both in Fig. 3(a) and 3(b), considering the one-electron labels and the values obtained for pole strengths, the leading ($S1$) correlation band seems to form a reversed image of the main band (M), an observation which nicely reflects their

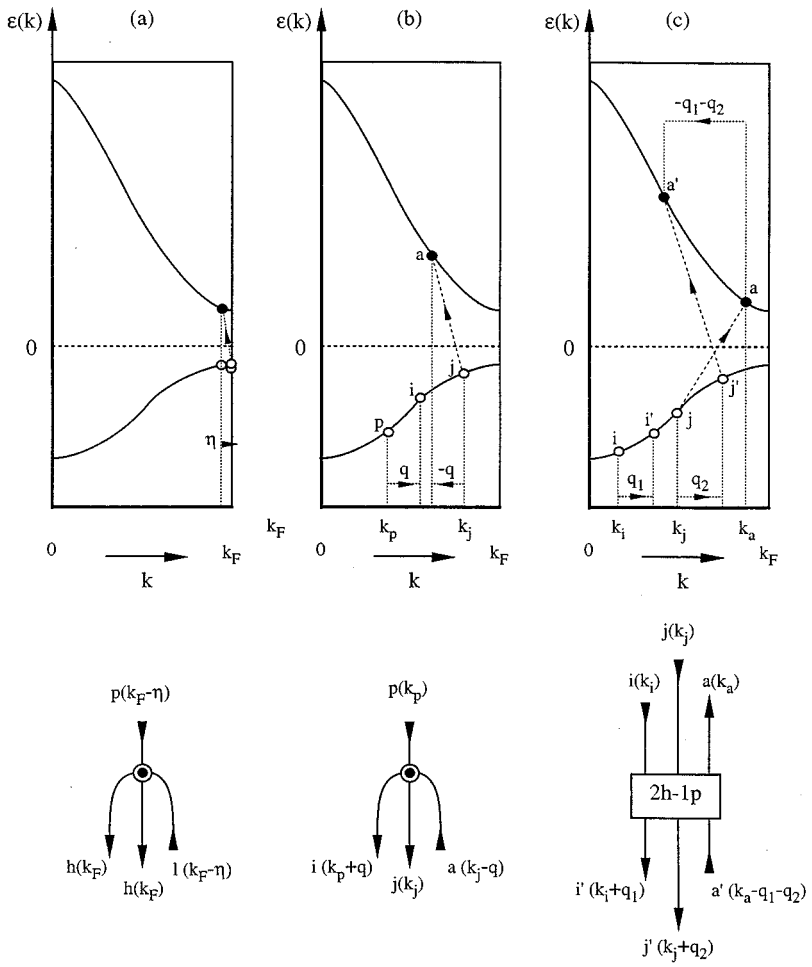

FIG. 4. Band-structure extrapolation, in a two bands model, of the observed (a) and (b) $1h/2h$-$1p$ and (c) $2h$-$1p/2h$-$1p$ configuration interactions (top) together with the permitted flows of momenta in the related coupling amplitudes, sketched (bottom) using diagrams introduced in Refs. 19, 23, or 47. The screened dot vertex (a) and (b) corresponds to the ADC (3) $1h/2h$-$1p$ coupling amplitudes $U^{-}_{p,ija}$ Refs. 26a, 47, whereas (c) the $2h$-$1p$ kernel accounts for the renormalization of the self-energy in terms of the $2h$-$1p/2h$-$1p$ coupling amplitudes $C^{-}_{ija,i'j'a'}$ Refs. 19, 23. In Fig. 3(a), η accounts for an infinitely small transfer of momentum accompanying the particle-hole excitation, which can be regarded as virtually vertical. In this figure, $h(k_F)$ and $l(k_F)$ correspond to the highest occupied and lowest unoccupied levels, at the edge (k_F) of the first Brillouin zone. (i,j: occupied band indices; a,b: virtual band indices.)

competition for intensity. From the composition of the associated eigenvector, the shake-up lines in the $S1$ band can be shown to essentially borrow their intensity from their mirror line in the main band, as a result of strong $1h/2h$-$1p$ interactions. Interestingly in Fig. 3(b), the $S2$ shake-up band displays a pole strength profile very similar to that found for the main band, and tends to form a mirror image of the $S1$ band. The $S2$ band can itself be regarded as a satellite of the $S1$ band, finding its origin in $2h$-$1p/2h$-$1p$ configuration interactions.

The features displayed in Fig. 3(b) are essentially retained for larger semiconducting hydrogen chains [e.g., H_{24} in Fig. 3(c)], although the pole strength distribution complicates quickly with system size. This behavior relates to the rapidly increasing number of possibilities for multistate configurations. In spite of this, however, one can readily distinguish several overlapping shake-up bands in Fig. 3(c), extending far beyond the high-energy border (at about 20.5 eV) of the remains of the primary band. Configuration interactions tend quite naturally to disfavor the shake-up states of highest energy, which explains the overall decrease observed with the intensity of shake-up lines with increasing binding energies, and relatedly the recovering of single-hole lines at the bottom of the valence band.

From the composition of the corresponding eigenvector in Eq. (22), the shake-up transition at the top of the correlation region is unsurprisingly always found to relate essentially to the $\mathrm{HOMO}^{-2}\mathrm{LUMO}^{+1}$ configuration. An analysis of the eigenvector also shows that, in the case of the hydrogen chains with bond lengths of 1.4 and 1.5 a.u., this shake-up line always borrows its intensity from the $(\mathrm{HOMO}-1)^{-1}$ single-hole configuration. When dealing with hydrogen chains of the semiconducting type [Figs. 3(b) and 3(c)], the $\mathrm{HOMO}^{-2}\mathrm{LUMO}^{+1}$ configuration state falls nearly at the upper edge of the main band, among the one-hole configurations corresponding to the outermost orbitals. These configurations interact strongly, yielding at that energy a severe depletion of intensity in the main band, and a very intense shake-up line.

Extrapolated to a band-structure description and as illustrated in Fig. 4(a) for a two-bands model, the $(\mathrm{HOMO}-1)^{-1}/\mathrm{HOMO}^{-2}\mathrm{LUMO}^{+1}$ splitting would relate to the interaction of a hole frozen in a one-electron state just nearby the top of the valence band with the $2h$-$1p$ state resulting from the ionization of the highest occupied electronic level, together with a vertical excitation over the fundamental gap, at the upper edge of the first Brillouin zone. In Fig. 4(a), the ADC (3) coupling amplitude corresponding to this $1h/2h$-$1p$ interaction is also displayed using Feynman diagrams, together with the permitted flows of momenta. Owing to translational symmetry constraints, an infinitely small transfer of momentum (η) has to obviously accompany the particle-hole excitation.

For ionization of electrons at higher binding energies, most of the induced particle-hole excitations imply a transfer of momentum (q), as shown in Fig. 4(b). The corresponding

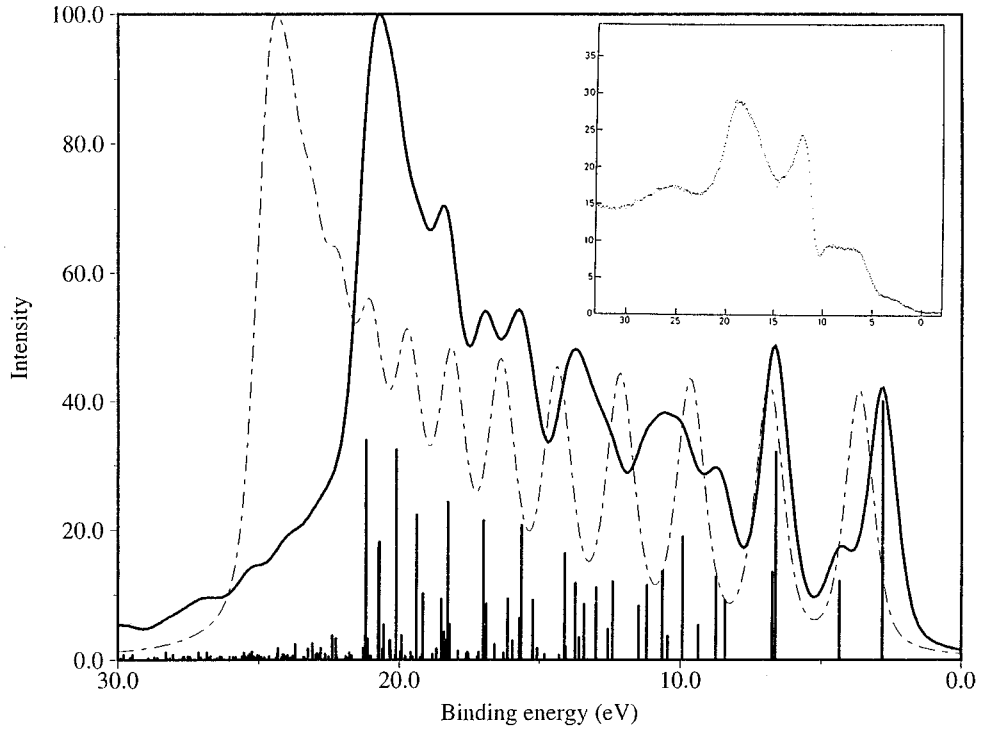

FIG. 5. Convoluted spectra (FWHM=1.2 eV) obtained from the results of (dashed-dotted line) HF and (full line) ADC (3) calculations, the latter being also displayed as a spike spectrum, for the H_{28} chain with bond lengths of 1.4 and 1.5 a.u. The insert shows the experimental XPS spectrum recorded on polyacetylene Ref. 14.

coupling amplitude therefore relates to a scattering of the created hole within the valence band as a result of correlation effects in the cation, together with an oblique electron transition across the fundamental gap. Owing to translational symmetry constraints, a vertical excitation ($q=0$) in our two bands model is possible only if the scattered hole [in state $\phi_i(k_p+q)$] remains frozen in its original state $\phi_r(k_p)$. As in this case, there is no charge oscillations, and this particular situation typically accounts for pure (orbital) relaxation effects. From Fig. 4(b), it is clear that for an infinitely large and periodic system, these relaxation states occur as singular cases in a continuum of correlation states, described by scanning all possible values for momenta.

As observed in Figs. 3(b) and 3(c), and as inferred from Fig. 4(b), shake-up solutions multiply quickly at higher binding energies, yielding multistate configuration interactions and further splitting into several series of satellites. In a band-structure picture, these interactions relate to a scattering [Fig. 4(c)] of the two-hole and one-particle states within the valence and conduction bands, respectively, which this time involves two independent variables for momentum transfer (q_1 and q_2).

C. Role of satellites in convoluted spectra

In Fig. 5, we compare the convoluted HF and ADC (3) spectra of a semiconducting H_{28} chain, with bond lengths of 1.4 and 1.5 a.u. From their overall aspect, and, in particular, from the appearance of a huge and intense peak at the bottom of the valence band, the HF and ADC (3) spectra of this chain present some similarity. In spite of this similarity, however, the underlying physics is very different.

In the HF case, the peak at about 24 eV results from a strong accumulation of one-electron levels in that energy region, yielding a characteristic and abrupt rise of intensity at the high-binding-energy border of the valence band. Additional and regularly distributed peaks can be distinguished at lower binding energies, each relating to a canonical one-particle state. As contrasted with the HF results and in analogy with simpler Green's-function calculations on extended chains,[7,27] the ADC (3) spectrum is shifted to lower binding energies and contracted on a smaller energy scale. As already mentioned, this overall behavior is due to the exaltation of the correlation effects in the final state (i.e., electron pair relaxation) with the inner character of the ionized levels.

As compared with the HF spectrum, the ADC (3) spectrum presents also a striking dissimilarity with its fuzzy and smoothened aspect. Except for the two peaks at the top of the convoluted band, the peaks emerging from the middle part of the ADC (3) simulation barely reminds us of those found in the HF spectrum. Very striking also is a net broadening of the peak at the high-binding-energy border of the main band (at 20 eV). This broadening is the outcome of an overlap between a few surviving one-electron lines with a large and poorly structured correlation tail, extending far beyond 30 eV.

In Fig. 5, we also compare the convoluted HF and ADC (3) spectra of the semiconducting H_{28} chain to the x-ray photoelectron spectrum (XPS) of polyacetylene,[14] in order to illustrate the role played by satellite structures in the photoionization spectra of conjugated polymers. This comparison relies on a firmly established tradition in condensed-matter physics,[41] and is justified in regards with the HF values obtained for the fundamental band gap (Table I), and with the alternation of the one-electron density. In close analogy with the ADC (3) convoluted spectrum of the hydrogen chain, a large and symmetric peak, extending in between 15 and 22 eV, is found in the inner valence part of the x-ray photoionization spectrum of polyacetylene.[14] By comparison, calcu-

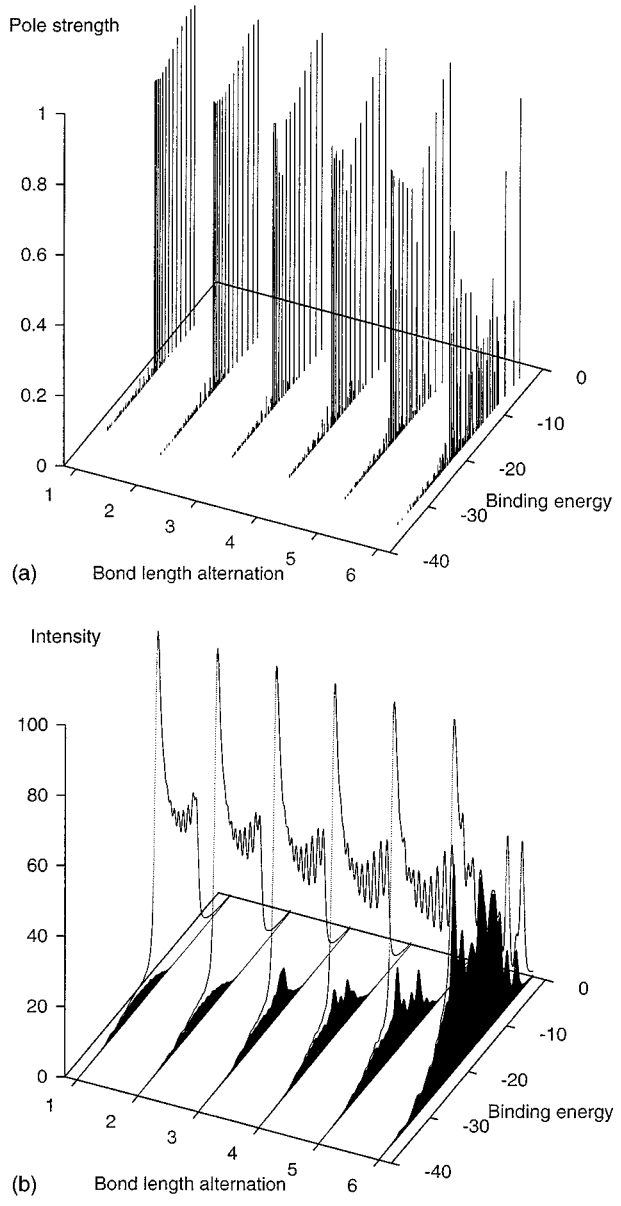

FIG. 6. Dependence of (a) the pole strength profile or (b) the convoluted spectra together with the contributions arising from shake up, superimposed as shaded spectra on the full result, displayed for different bond-length alternations of a H_{28} chain. 1: 1.4/2.0 a.u.; 2: 1.4/1.9 a.u.; 3: 1.4/1.8 a.u.; 4: 1.4/1.7 a.u.; 5: 1.4/1.6 a.u.; 6: 1.4/1.5 a.u.

lations based on a quasiparticle picture yield,[47,48] as with the HF calculations on the semiconducting hydrogen chains, a sharper and more assymmetric peak in that energy region.

D. Conditions precluding a contamination of main bands by shake-up lines

In Figs. 6(a) and 6(b), we present the spike and convoluted spectra for a H_{28} chain computed at different bond distances between the H_2 monomer units. In these figures, one can easily follow the growing contamination of the spectrum by shake-up bands, as one reduces the bond-length alternation. This contamination spreads from the high-binding-energy border of the main band up to nearly its low-binding-energy edge, in direct relationships with the decreasing band gap.

We noticed that the zeroth-order estimate for the energy threshold of a shake-up transition, i.e., $\Delta_S^0=\epsilon_{\mathrm{LUMO}}-2\epsilon_{\mathrm{HOMO}}$ marks the bifurcation range between the one-particle and many-body parts of the ionization spectrum. Below that threshold, the dispersion of intensity into secondary lines directly relates to the strength of relaxation effects, and therefore increases[7,8b] with increasing binding energy. Above Δ_S^0, one has to consider the probability of shake-up transitions, decreasing with increasing binding energy, together with the strength of the interaction between the main (one-hole) and secondary (two-holes, one-particle) configurations of the ionized system. The strongest configuration interactions with shake up are likely to operate in an energy region centered on Δ_S^0. Hence, the intensity in the main band does increase again with increasing binding energy above that threshold, as observed previously.

Therefore, Δ_S^0 has naturally to correspond to the strongest depletion of intensity in the main band, and relatedly to the highest extremum in the shake-up structures. As shown in Table II, the zeroth-order energy threshold for a shake-up transition is indeed very generally found in the vicinity of the most severe depletion of intensity in the main band and of the most intense shake-up structure in the correlation tail. The energy locations of these features are denoted Δ_D and Δ_C, respectively.

This observation relates to the delocalization properties of canonical states in extended chains, yielding bielectron integrals and thereby $1h/2h\text{-}1p$ and $2h\text{-}1p/2h\text{-}1p$ coupling amplitudes scaling like N_0^{-1}, with N_0 the number of monomer units. When the size of the system tends to infinity, the number of shake-up possibilities tends to become infinitely large, whereas the coupling amplitudes tend to become infinitely small (i.e., the coupling amplitudes tend to build infinitely large matrices $U^{\pm}$ and $C^{\pm}$, with infinitely small elements). For an infinite system, the poles of the self-energy (8) therefore strictly reduce to the zeroth-order estimates for shake-on $[K^{+}_{iab,i'a'b'}=\delta_{ii'}\delta_{aa'}\delta_{bb'}(\epsilon_i-\epsilon_a-\epsilon_b)]$ or shake-up $[K^{-}_{ati,a'i'j'}=\delta_{aa'}\delta_{ii'}\delta_{jj'}(\epsilon_a-\epsilon_i-\epsilon_j)]$ energies (a,b: unoccupied indices; i,j: occupied indices).

Along the same lines, a zeroth-order value of 10.86 eV for the shake-up energy threshold of polyacetylene can be readily calculated from the values obtained by Suhai[44] for the first ionization potential and fundamental gap. Similarly, a value of 27.69 eV for Δ_S^0 is found in the case of polyethylene. By extrapolation of our argumentation, the greater part of the photoionization intensity can therefore be attributed to main lines in the latter case, whereas a significant contamination by shake-up lines can be expected in the lower half part of the outer (C $2p$+H $1s$) valence band of polyacetylene, together with a complete breakdown of the one-particle picture in the inner (C $2s$) valence region.

This observation and explanations are consistent with the $2h\text{-}1v$ CI calculations carried out on finite polyenes (C_8H_{10},$C_{10}H_{12}$), by Fronzoni *et al.*,[16] indicating a severe breakdown of the one-particle picture for the inner valence band of polyacetylene, together with a possible irruption of shake-up lines into the outer valence region. In this case, however, the fragmentation of the main band into satellites

TABLE II. Comparison of the zeroth-order estimate for the energy threshold of a shake-up transition (Δ_S^0) with the energy locations (together with the corresponding pole strength) of the depletion center of intensity in the main band (Δ_D) and of the most intense structure (Δ_C) in the correlation tail (energies in eV). The * denotes that shake-up lines of comparable intensity are also found in the correlation tail, beyond the high-binding-energy edge of the main band.

NH	Alternation	Δ_S^0	Δ_D (eV)	Δ_C (eV)
(a)	1.4/1.5	23.445	19.28 (0.573)	23.13 (0.379)
8	1.4/1.5	17.083	12.65 (0.426)	16.19 (0.509)
12	1.4/1.5	13.621	9.49 (0.358)	12.44 (0.562)
16	1.4/1.5	11.359	7.75 (0.306)	10.21 (0.599)
20	1.4/1.5	9.728	6.28 (0.276)	8.64 (0.619)
24	1.4/1.5	8.468	5.34 (0.245)	7.49 (0.632)
28	1.4/1.5	7.443	4.34 (0.237)	6.62 (0.639)
(b)				
4	1.4/1.8	26.240	18.87 (0.856)	25.28 (0.097)
8	1.4/1.8	21.823	17.69 (0.804)	19.14 (0.091)
12	1.4/1.8	19.780	18.95 (0.736)	19.16 (0.149)
16	1.4/1.8	18.670	18.36 (0.783)	19.81 (0.096)
20	1.4/1.8	17.976	17.96 (0.783)	19.93 (0.089)
24	1.4/1.8	17.519	17.67 (0.780)	18.44 (0.097)
28	1.4/1.8	17.201	17.46 (0.632)	17.48 (0.184)
			16.55 (0.778)	18.31 (0.140)
32	1.4/1.8	16.972	17.250 (0.752)	19.76 (0.181)
36	1.4/1.8	16.801	18.35 (0.495)	18.36 (0.306)
			16.34 (0.776)	17.85 (0.056)
40	1.4/1.8	16.671	17.0 (0.500)	18.29 (0.057)
(c)				
28	1.4/1.5	7.443	4.343 (0.237)	6.62 (0.639)
28	1.4/1.6	14.837	13.99 (0.306)	13.986 (0.487)
28	1.4/1.7	16.127	15.56 (0.624)	16.605 (0.146)
28	1.4/1.8	17.201	17.46 (0.631)	17.48 (0.184)
			16.55 (0.778)	18.31 (0.140)
28	1.4/1.9	18.121	18.143 (0.809)	17.954 (0.041)*
28	1.4/2.0	18.909	18.556 (0.828)	18.723 (0.029)*

seems less pronounced than with our present ADC (3) calculations on hydrogen chains with a similar band gap. This could probably be the result of the loss of size-consistency inherent to truncated CI expansions and of the restriction of the virtual state to the valence space generated in a minimal basis.

E. The role of correlation effects in the ground-state wave function

As a last point, we compare in Fig. 7 the above discussed ADC (3) results for hydrogen chains of the semiconducting type with ADC (2) calculations. In the ADC (2) scheme, the vectors of coupling amplitudes $U^{\pm}$ are obtained to first order in correlation, whereas the ADC (3) scheme also incorporates second-order correlation corrections to the reference ground-state wave function. The ADC (2) and ADC (3) results are qualitatively consistent, even for the chains with the more strongly pronounced metallic character. As compared with ADC (2), however, the many-body corrections in the ADC (3) scheme tend overall to strengthen the breakdown of the one-particle picture for the ionization process. This difference relates to a narrowing of the fundamental quasiparticle band gap of semiconducting polymers[44] under the inclusion of electronic correlation effects in the ground state, yielding larger $1h/2h\text{-}1p$ coupling amplitudes. This last comparison strengthens the reliability of the conclusions obtained, which could be readily transposed to a wide range of insulating or semiconducting polymers with a HF band gap larger than 5.0 eV.

V. SUMMARY AND OUTLOOK FOR THE FUTURE

The calculations and analysis presented in this paper establish a link between many-body molecular quantum mechanics and condensed-matter physics. They illustrate the importance of satellite bands in the photoionization spectra of extended systems with low band gap, an aspect of band-structure theory which has been largely overlooked until now.

In this paper, we have computed the ionization spectra of model hydrogen chains, with different bond-length alterna-

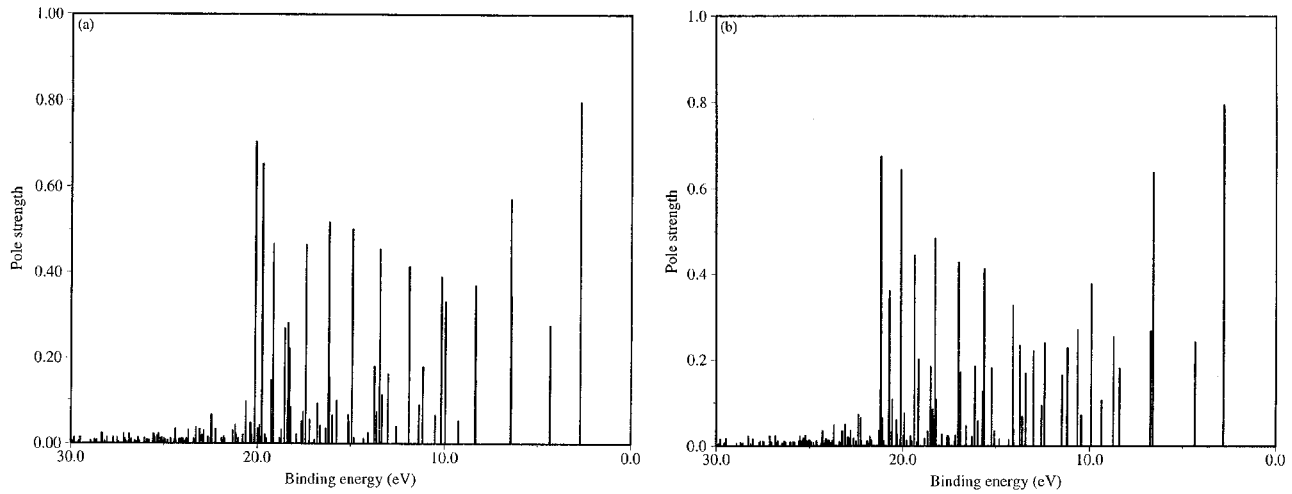

FIG. 7. Comparison of the (a) ADC (2) results with (b) the ADC (3) results obtained for a semiconducting H_{28} hydrogen chain, with alternating bond lengths of 1.4 and 1.5 a.u.

tions and as a function of chains length. Our main goal was to investigate the construction of satellite bands in two extreme situations i.e., for an insulating and for a semiconducting polymer chain. Since the formation of satellite states essentially depends on many-body effects, use has been made of calculations which account for electronic correlation and relaxation effects, as well as for multistate configuration interactions. The method which has been considered is an algebraic diagrammatic construction scheme (ADC) of the one-particle Green's function, which is correct through third order in correlation. It has been recently augmented by a block Lanczos algorithm, which makes this method applicable to larger clusters. In comparison with standard CI treatments, this approach has major advantages for numerical applications of extended systems, in the form of a systematic *compactness* of the configuration spaces, and in regards with the *size consistency* and thereby *size intensivity* of the computed transition energies and moments.

Satellite structures in the ionization spectra of large systems are, by far, much more difficult to investigate than one-particle lines, since the number of $2h\text{-}1p$ shake-up solutions increase as $(N_0)^3$, with N_0 the number of monomer units, whereas the corresponding $1h/2h\text{-}1p$ and $2h\text{-}1p/2h\text{-}1p$ coupling amplitudes tend to scale as $(N_0)^{-1}$ in the limit of an infinite system. In spite of this, evidence has been found in this study for an organization of shake-up lines into a regular band structure, in direct relationships with the developing translational symmetry constraints in clusters converging onto a stereoregular polymer limit. From the distribution of lines and intensities, it is even possible to distinguish the satellites due to a single $1h/2h\text{-}1p$ configuration interaction from those arising from multistate $2h\text{-}1p/2h\text{-}1p$ interactions.

When dealing with insulating hydrogen chains, the shake-up contamination remains limited to a small part of the ionization spectrum, at the high-binding-energy edge of the valence region. In this case, the correlation tail saturates rather quickly to its asymptotic form, with respect to the size of the chains, as a result of a suitable (i.e., *size-consistent*) balance[26] between the multiplicity of shake-up solutions and the scaling properties of coupling amplitudes. On the contrary, for systems of the semiconducting type (with a HF band gap of the order of 5 eV), a virtually complete fragmentation of main bands into satellites is observed below the zeroth-order estimate for the energy threshold of a shake-up transition (Δ_S^0), namely, the $\mathrm{HOMO}^{-2}\mathrm{LUMO}^{+1}$ transition. The amplitude of this fragmentation increases under the inclusion of electronic correlation in the ground-state reference function, owing to a narrowing of the quasiparticle band gap.

As shown in this paper, the energy threshold Δ_S^0 provides a simple criterium to evaluate the range of reliability of the one-particle picture for the ionization process, an essential question in the assessment of configurational or conformational signatures in the photoionization spectra of extended systems. Considering energetics only, it is quite obvious that Δ_S^0 should always fall in the vicinity of the most severe depletion of intensity in the primary bands and of the most intense satellite structure. Nonetheless, in more realistic systems with one-particle levels belonging to different shells, one should also consider the modulation of the competition for intensity between primary and secondary lines by their coupling amplitudes, which depend sensitively on the localization properties of the involved orbitals.

A main conclusion is that although not necessarily apparent from experiment alone, the structures observed in the ionization spectra of semiconducting polymers can be essentially due to correlation and not related to a one-particle picture at all. More care should be exercised when interpreting these spectra. By extrapolation of studies conducted during the past two decades on a large range of molecules,[11] strong many-body effects can also be expected in the inner valence spectrum of polymers containing easily polarizable bonds or lone pairs such as polysilanes, polyoxymethylene, polyoxyethylene, polyacrylonitrile . . . . Many more calculations, of the type which has been presented here, are, therefore, needed for other large oligomers. A crystal orbital version of the ADC scheme, fully exploiting translational symmetry for infinite periodic systems, is also clearly desirable.

Along the same lines, it is usually agreed that the one-particle picture for ionization is applicable on metallic systems. An open and highly challenging problem, yet to be studied, is following the evolution of satellite bands when the semiconducting phase presented here evolves to a strongly correlated metallic phase.

ACKNOWLEDGMENTS

M. Deleuze is grateful to the FNRS, the Belgian National Fund for Scientific Research, for his position as a Senior Research Assistant for the ''Laboratoire de Chimie Théorique Appliquée'' at the ''Facultés Universitaires Notre-Dame de la Paix (FUNDP),'' Namur (Belgium). He is indebted to Professor J. Delhalle (FUNDP, Namur, Belgium) and Professor Barry T. Pickup (University of Sheffield, UK) for continuous support and collaboration in the field of extended systems and Green's-function theory, respectively. He would also like to gratefully acknowledge Dr. D. H. Mosley (FUNDP, Namur, Belgium) for providing the band-structure data used for polyethylene.

*Present address: Laboratoire de Chimie Théorique Appliquée, Facultés Universitaires Notre-Dame de la Paix, Rue de Bruxelles 61, B5000 Namur, Belgium.

[1] (a) J. Delhalle, J.-M. André, S. Delhalle, J. J. Pireaux, R. Caudano, and J. J. Verbist. J. Chem. Phys. **60**, 595 (1974); (b) J. Delhalle, Chem. Phys. **5**, 306 (1974); (c) J. J. Pireaux, J. Riga, R. Caudano, J. J. Verbist, J.-M. André, J. Delhalle, and S. Delhalle, J. Electron Spectrosc. Relat. Phenom. **5**, 531 (1974); (d) S. Delhalle, J. Delhalle, Ch. Demanet, and J.-M. André, Bull. Soc. Chim. Belg. **84**, 1071 (1975); (e) J. J. Pireaux, J. Riga, R. Caudano, J. J. Verbist, J. Delhalle, S. Delhalle, J.-M. André and Y. Gobillon, Phys. Scr. **16**, 329 (1977); (f) J. Delhalle, R. Montigny, Ch. Demanet, and J.-M. André, Theor. Chim. Acta **50**, 343 (1979).

[2] (a) P. Boulanger, R. Lazzaroni, J. Verbist, and J. Delhalle, Chem. Phys. Lett. **129**, 275 (1986); (b) P. Boulanger, J. Riga, J. Verbist, and J. Delhalle, Macromolecules **21**, 173 (1989); (c) G. Hennico, J. Delhalle, G. Boiziau, and G. Lecayon, J. Chem. Soc.

Faraday Trans. **86**, 1025 (1990); (d) P. Boulanger, C. Magermans, J. Verbist, J. Delhalle, and D. S. Urch, Macromolecules **24**, 2757 (1991).

[3] For a review, see, e.g., J.-M. André, Adv. Quantum Chem. **12**, 65 (1980).

[4] (a) J.-L. Brédas, Chem. Phys. Lett. **115**, 119 (1985); (b) W. R. Salaneck, C. R. Wu, J.-L. Brédas, and J. J. Ritsko, *ibid*. **127**, 88 (1986); (c) J.-L. Brédas and W. R. Salaneck, J. Chem. Phys. **85**, 2219 (1986); (d) R. Lazzaroni, A. de Bryck, Ch. Debraisieux, J. Riga, J. Verbist, J.-L. Brédas, J. Delhalle, and J.-M. André, Synth. Met. **21**, 189 (1987); (e) R. Lazzaroni, J. Riga, J. Verbist, J.-L. Brédas, J. Delhalle, and F. Wudl, J. Chem. Phys. **88**, 4257 (1988); (f) W. R. Salaneck, O. Inganäs, B. Thémans, J. O. Nilsson, B. Sjögren, J. E. Österholm, J.-L. Brédas, and S. Svensson, *ibid*. **88**, 4613 (1988); (g) E. Orti and J. L. Brédas, *ibid*. **89**, 1009 (1988).

[5] (a) J. V. Ortiz, J. Am. Chem. Soc. **110**, 4522 (1988); (b) Macromolecules **21**, 1189 (1988); (c) J. Chem. Phys. **94**, 6064 (1991); (d) Macromolecules **26**, 7282 (1993).

[6] J. Delhalle and M. Deleuze, J. Mol. Struct. (Theochem.) **261**, 187 (1992).

[7] (a) M. Deleuze, J.-P. Denis, J. Delhalle, and B. T. Pickup, J. Phys. Chem. **97**, 5115 (1993); (b) M. Deleuze, J. Delhalle, and B. T. Pickup, Chem. Phys. **175**, 427 (1993); (c) M. Deleuze, J. Delhalle, B. T. Pickup, and S. Svensson, J. Am. Chem. Soc. **116**, 10 715 (1994); (d) M. Delueze, J. Delhalle, D. H. Mosley, and J.-M. André, Phys. Scr. **51**, 111 (1995).

[8] (a) J. Delhalle, J. Riga, J. P. Denis, M. Deleuze, and M. Dosière, Chem. Phys. Lett. **210**, 21 (1993); (b) J. Riga, J. Delhalle, M. Deleuze, J. J. Pireaux, and J. Verbist, Surf. Int. Anal. **22**, 507 (1994).

[9] A. S. Duwez, M. Deleuze, J. Riga, J. Ghijsens, and J. Delhalle (unpublished).

[10] (a) W. R. Salaneck, H. R. Thomas, R. W. Bigelow, C. B. Duke, E. W. Plummer, J. J. Heeger, and A. G. MacDarmid, J. Chem. Phys. **72**, 3674 (1980); (b) R. Schultz, A. Schweig, and A. Zittlau, J. Am. Chem. Soc. **105**, 2980 (1983); (c) M. P. Keane, S. Svensson, A. Naves de Brito, N. Correia, S. Lunell, B. Sjögren, O. Inganes, and W. R. Salaneck, J. Chem. Phys. **93**, 6357 (1990); (d) B. Sjögren, A. Naves de Brito, S. Lunell, B. Wannberg, U. Gelius, and S. Svensson, J. Electron Spectrosc. **59**, 161 (1992); (e) B. Sjögren, S. Svensson, A. Naves de Brito, N. Correia, M. P. Keane, C. Enkvist, and S. Lunell, J. Chem. Phys. **96**, 6389 (1992); (f) A. Lisini, M. P. Keane, S. Lunell, N. Correia, A. Naves de Brito, and S. Svensson, Chem. Phys. **169**, 379 (1993).

[11] (a) L. S. Cederbaum, G. Hohlneicher, and W. Von Niessen, Chem. Phys. Lett. **18**, 503 (1973); (b) L. S. Cederbaum, *ibid*. **25**, 562 (1974); (c) L. S. Cederbaum, Mol. Phys. **28**, 479 (1974); (d) L. S. Cederbaum, J. Schirmer, W. Domcke, and W. Von Niessen, Int. J. Quantum Chem. **14**, 593 (1978); (e) L. S. Cederbaum, W. Domcke, J. Schirmer, W. Von Niessen, G. H. F. Diercksen, and W. P. Kraemer, J. Chem. Phys. **69**, 1591 (1978); (f) J. Schirmer, W. Domcke, L. S. Cederbaum, and W. Von Niessen, J. Phys. B **11**, 1901 (1978); (g) W. Domcke, L. S. Cederbaum, J. Schirmer, and W. Von Niessen, Chem. Phys. **40**, 171 (1979); (h) J. Schirmer, W. Domcke, L. S. Cederbaum, W. Von Niessen, and L. Åsbrink, Chem. Phys. Lett. **61**, 30 (1979); (i) W. Von Niessen and G. H. F. Diercksen, J. Electron Spectrosc. Relat. Phenom. **20**, 95 (1980); (j) L. S. Cederbaum, J. Schirmer, W. Domcke, and W. Von Niessen, Adv. Chem. Phys. **65**, 115 (1986).

[12] (a) R. W. Bigelow, Int. J. Quantum Chem. **19**, 35 (1986); (b) M. Deleuze, P. Horeczky, J. Delhalle, and B. T. Pickup, Int. Chem. Symp. **26**, 31 (1992). (c) G. Fronzoni, G. De Alti, P. Decleva, and A. Lisini, Chem. Phys. **195**, 171 (1995).

[13] M. Deleuze and L. S. Cederbaum (unpublished).

[14] M. P. Keane, A. Naves de Brito, N. Correia, S. Svensson, L. Karlsson, B. Wannberg, U. Gelius, S. Lunell, W. R. Salaneck, M. Lödlung, D. B. Swanson, and A. G. Mac Diarmid, Phys. Rev. B **45**, 6390 (1992).

[15] C.-M. Liegener, Phys. Rev. B **47**, 1607 (1993).

[16] G. Fronzoni, P. Decleva, A. Lisini, and G. De Alti, J. Electron Spectrosc. **69**, 207 (1994).

[17] A. L. Fetter and J. D. Walecka, *Quantum Theory of Many Particle Systems* (McGraw-Hill, New York, 1971).

[18] J. Linderberg and Y. Öhrn, *Propagators in Quantum Chemistry* (Academic, New York, 1973).

[19] L. S. Cederbaum and W. Domcke, Adv. Chem. Phys. **36**, 205 (1977).

[20] Y. Öhrn and G. Born, Adv. Quantum Chem. **13**, 1 (1981).

[21] M. F. Herman, K. F. Freed, and D. L. Yeager, Adv. Chem. Phys. **48**, 1 (1981).

[22] (a) B. T. Pickup and O. Goscinski, Mol. Phys. **26**, 1013 (1973); (b) G. D. Purvis and Y. Öhrn, J. Chem. Phys. **62**, 2045 (1975); (c) P. Jørgensen and J. Simons, *ibid*. **63**, 5302 (1975); (d) J. Baker and B. T. Pickup, Chem. Phys. Lett. **56**, 637 (1980); (e) J. Baker, Chem. Phys. **79**, 117 (1983).

[23] J. Schirmer and L. S. Cederbaum, J. Phys. B **11**, 1889 (1978).

[24] J. Schirmer, L. S. Cederbaum, and O. Walter, Phys. Rev. A **28**, 1237 (1983).

[25] (a) J. Schirmer, Phys. Rev. A **43**, 4647 (1991); (b) F. Mertins and J. Schirmer (unpublished); (c) F. Mertins, Ph.D. thesis, Heidelberg, Germany, 1995.

[26] (a) M. Deleuze, Ph.D. thesis, FUNDP-Namur, Belgium, 1993; (b) M. Deleuze, J. Delhalle, B. T. Pickup, and J.-L. Calais, Adv. Quantum Chem. **26**, 35 (1995); (c) M. Deleuze and B. T. Pickup, J. Chem. Phys. **102**, 8967 (1995).

[27] (a) M. Deleuze, J. Delhalle, and J.-M. André, Int. J. Quantum Chem. **41**, 243 (1992); (b) M. Deleuze, J. Delhalle, B. T. Pickup, and J.-L. Calais, Phys. Rev. B **46**, 15 668 (1992).

[28] (a) J. Goldstone, Proc. R. Soc. London, Ser. A **239**, 267 (1957); (b) J. Paldus and J. Cisek, Adv. Quantum Chem. **7**, 105 (1975); (c) V. Kvanicka, Adv. Chem. Phys. **36**, 345 (1977).

[29] N. H. March, W. H. Young, and S. Sampanthar, *The Many-Body Problem in Quantum Mechanics* (Cambridge University Press, Cambridge, 1967).

[30] A. D. Mattuck, *A Guide to Feynman Diagrams in the Many-Body Problem* (McGraw Hill, New York, 1967).

[31] M. Deleuze, M. K. Scheller, and L. S. Cederbaum, J. Chem. Phys. **103**, 3578 (1995).

[32] D. N. Zubarev, Usp. Fiz. Nauk. **71**, 71 (1960) [Sov. Phys. Usp. **3**, 320 (1960)].

[33] A. B. Migdal, *Theory of Finite Fermi Systems and Applications to Atomic Nuclei* (Wiley, New York, 1971).

[34] H.-G. Weikert, H.-D. Meyer, L. S. Cederbaum, and F. Tarantelli (unpublished).

[35] A. Ruhe, Math. Comput. **33**, 680 (1979).

[36] H.-D. Meyer and S. Pal, J. Chem. Phys. **91**, 6195 (1989).

[37] (a) G. Lanczos, J. Res. Natl. Bur. Stand. **45**, 255 (1950); (b) B. N. Parlett, *The Symmetric Eigenvalue Problem* (Prentice-Hall,

Englewood Cliffs, NJ, 1980); (c) J. K. Cullum and R. A. Willoughby, *Lanczos Algorithms for Large Symmetric Eigenvalue Computations* (Birkhuser, Boston, 1985).

[38] W. Von Niessen, J. Schirmer, and L. S. Cederbaum, Comput. Phys. Rep. **1**, 59 (1984).

[39] J. Schirmer and G. Angonoa, J. Chem. Phys. **91**, 1754 (1989).

[40] H.-G. Weikert and L. S. Cederbaum, Few Body Syst. **2**, 33 (1987).

[41] E.g., (a) M. Kertèsz, Phys. Rev. B **14**, 76 (1976); (b) F. E. Harris and J. Delhalle, Phys. Rev. Lett. **39**, 1340 (1977); (c) J. Delhalle and F. E. Harris, Theor. Chim. Acta **48**, 128 (1978); (d) S. Suhai and J. Ladik, J. Phys. C **15**, 4237 (1982); (e) W. Förner, J. Ladik, P. Otto, and J. Cizek, Chem. Phys. **97**, 251 (1985); (f) C.-M. Liegener and J. Ladik, Phys. Lett. **107A**, 79 (1985); (g) C.-M. Liegener, J. Phys. C **18**, 6011 (1985); (h) J. G. Fripiat, J.-M. André, J. Delhalle, and J.-L. Calais, Int. J. Quantum Chem. Symp. **25**, 603 (1991); (i) Y. J. Ye, W. Förner, and J. Ladik, Chem. Phys. **178**, 1 (1993); (j) S. Suhai, Phys. Rev. B **50**, 14 791 (1994).

[42] (a) A. K. McMahan, in *High-Pressure and Low-Temperature Physics*, edited by C. W. Chu and J. A. Woollam (Plenum, New York, 1978), p. 21; (b) J. van Kranendonk, *Solid Hydrogen* (Plenum, New York, 1983).

[43] (a) Data by Dr. D. H. Mosley, Computer Code PLH-93, Namur, Belgium; (b) D. H. Mosley, J.-G. Fripiat, B. Champagne, and J.-M. André, Int. J. Quantum Chem. Symp. **27**, 793 (1993).

[44] (a) S. Suhai, Chem. Phys. Lett. **96**, 619 (1983); (b) Int. J. Quantum Chem. **23**, 1239 (1983); (c) Phys. Rev. B **27**, 3506 (1983).

[45] M. W. Schmidt *et al.*, QCPE Bull. **10**, 52 (1990).

[46] I. Cacelli, R. Moccia, and V. Carrevetta, Theor. Chim. Acta **59**, 461 (1981).

[47] C.-M. Liegener, Chem. Phys. Lett. **167**, 555 (1990).

[48] M. Deleuze and B. T. Pickup (unpublished).